Supporting Information

Separating critical elements from NdFeB magnets with aminophosphonic acid functionalised 3D printed filters and their detailed structural characterisation

Emilia J. Virtanen,[a,c] Janne Yliharju,[b,c,e] Esa Kukkonen,[a,c] Tia Christiansen,[a] Eero Hulkko,[a,c,f] Minnea Tuomisto,[d] Arttu Miettinen,[b,c,e] Mika Lastusaari,[d] Ari Väisänen,[a] and Jani O. Moilanen*[a,c]

[a] Department of Chemistry, University of Jyväskylä, P.O. Box 35, FI-40014 Jyväskylä, Finland.
[b] Department of Physics, University of Jyväskylä, P.O. Box 35, FI-40014 Jyväskylä, Finland.
[c] Nanoscience Center, University of Jyväskylä, P.O. Box 35, FI-40014 Jyväskylä, Finland.
[d] Department of Chemistry, University of Turku, FI-20014 Turku, Finland
[e] School of Resource Wisdom, University of Jyväskylä, P.O. Box 35, FI-40014 Jyväskylä
[f] Department of Biological and environmental sciences, University of Jyväskylä, P.O. Box 35, FI-40014 Jyväskylä, Finland

Contents

Table S1 Adsorption percentages for the pure nylon-12 filter with 5% MSA as the background.

Fe	Nd	Dy	Pr	Co	B	Tb	Sm	Ho	Al	Cu
0.0 ± 0.0%	1.8 ± 1.0%	2.3 ± 0.3%	2.5 ± 0.1%	1.5 ± 0.6%	0.0 ± 0.0%	0.7 ± 0.8%	1.6 ± 1.1%	1.4 ± 0.7%	0.0 ± 0.0%	0.0 ± 0.0%

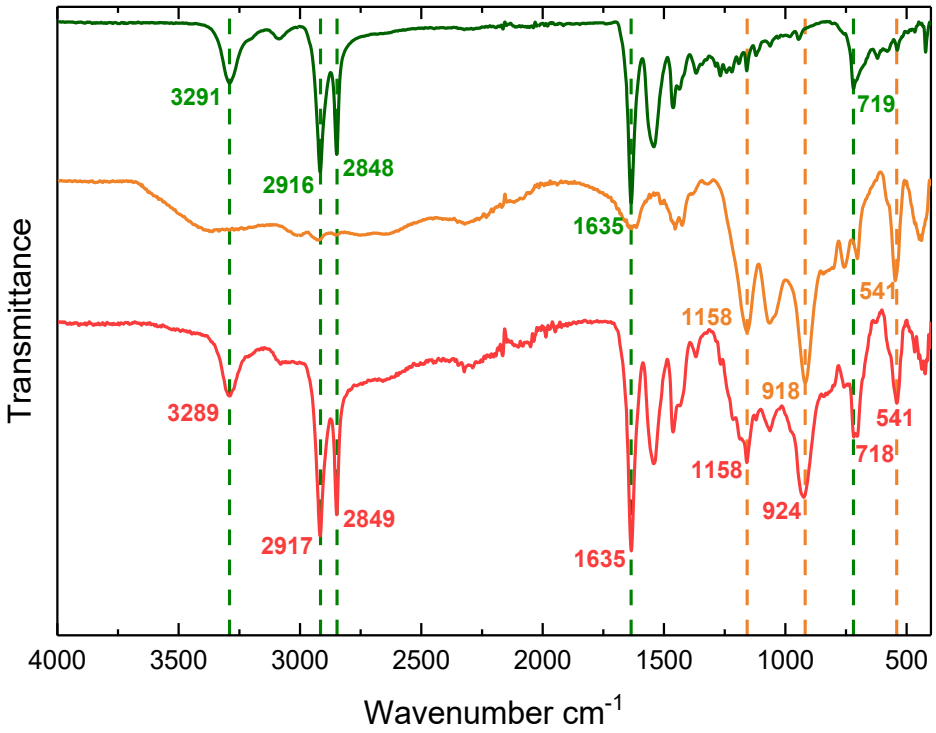

Figure S1 FTIR spectra of nylon-12 (green), Lewatit TP260 in H+ form (orange), and 30 wt% PA-TP260 (red).

Characterisation of the FTIR peaks: Characteristic peaks of nylon-12 arising from the NH stretch at 3291 cm^{-1} and CH_2 stretches at 2916 cm^{-1} and 2848 cm^{-1} and bending at 719 cm^{-1} is slightly shifted in the spectrum of the PA-TP260 as their positions are at 3289 cm^{-1}, 2917 cm^{-1}, 2849 cm^{-1}, and 718 cm^{-1}, respectively. No shift is observed for the C=O stretch at 1635 cm^{-1}. When FTIR spectra of Lewatit TP260 and the PA-TP260 filter are compared to each other, it can be seen that the positions of the peaks from the C-PO_3H_2 moiety at 1158 cm^{-1} (P=O), 918 cm^{-1} (P-OH), and 541 cm^{-1} (C-PO_3) remain the same, but the P-OH stretch is slightly shifted from 918 cm^{-1} to 924 cm^{-1} for the PA-TP260.[1–3]

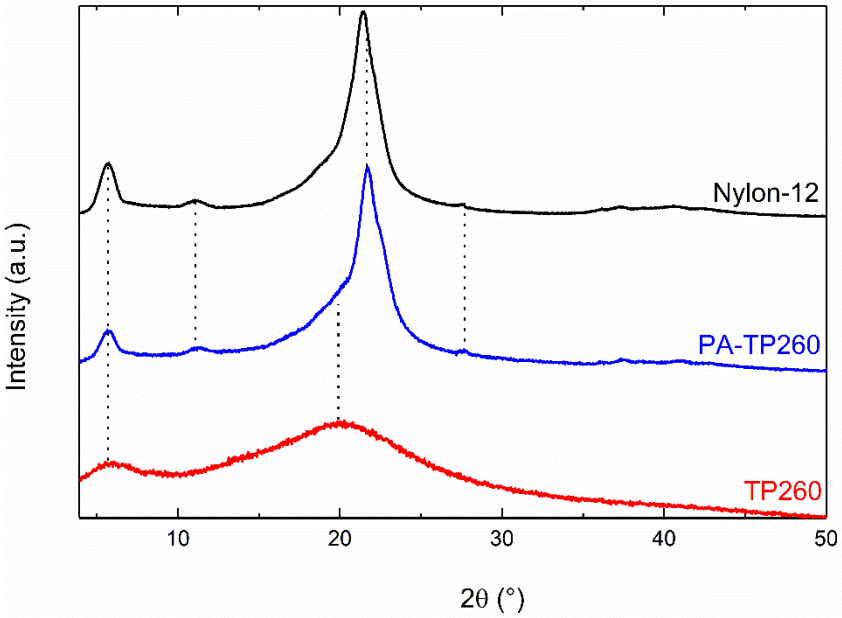

Figure S2 PXRD of nylon-12 (red), pure Lewatit TP260 (blue) and 3D printed filter containing a 30 wt% of TP260 (black).

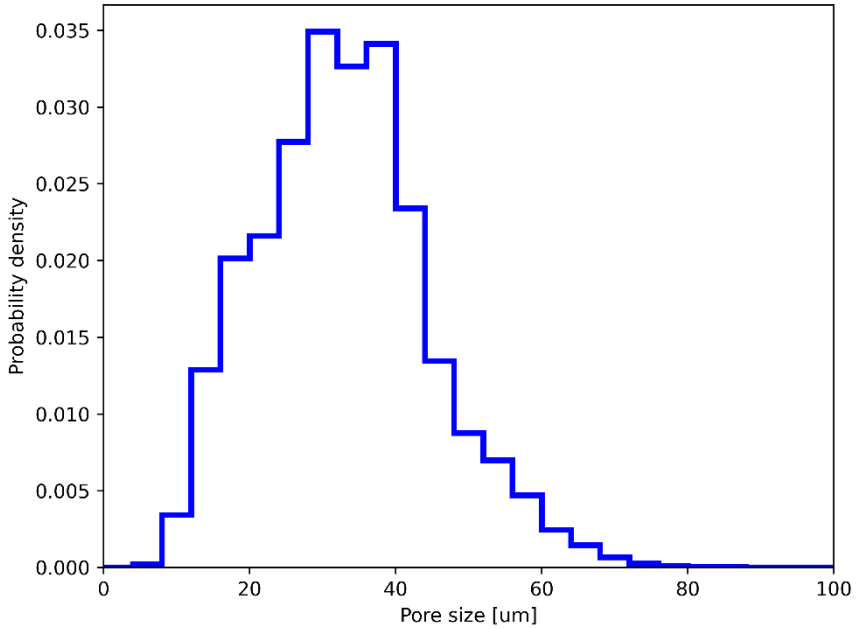

Figure S3 Pore size distribution for the 3D printed 30 wt% PA-TP260 filter.

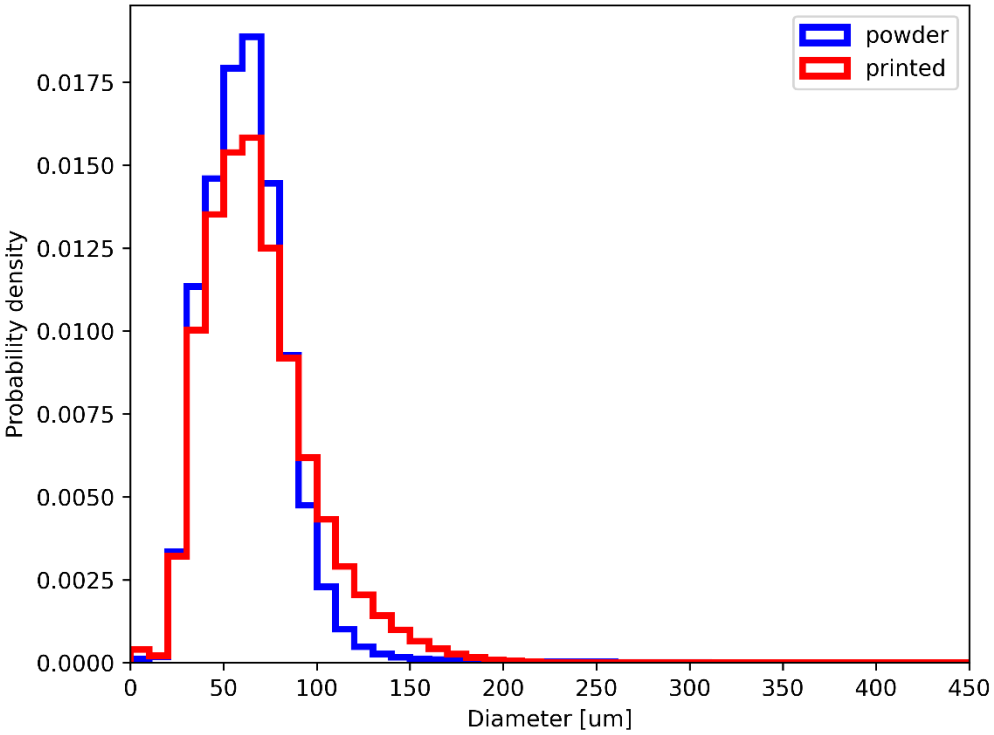

Figure S4 Particle size distribution for the unprinted 30 wt% PA-TP260 powder (blue) and 3D printed 30 wt% filter (red).

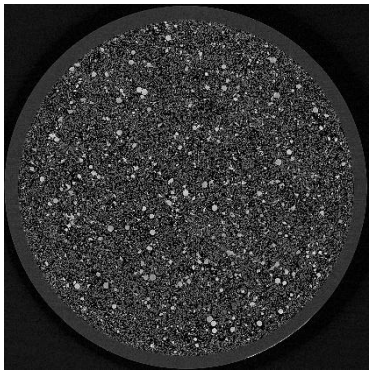

Figure S5 A tomographic cross-section of a PA-TP260 filter with a voxel size of 6.6 µm × 6.6 µm × 6.6 µm inside the syringe. The darker areas represent the nylon-12 particles, while the lighter areas represent the additives, which appear to be uniformly distributed in the filter material.

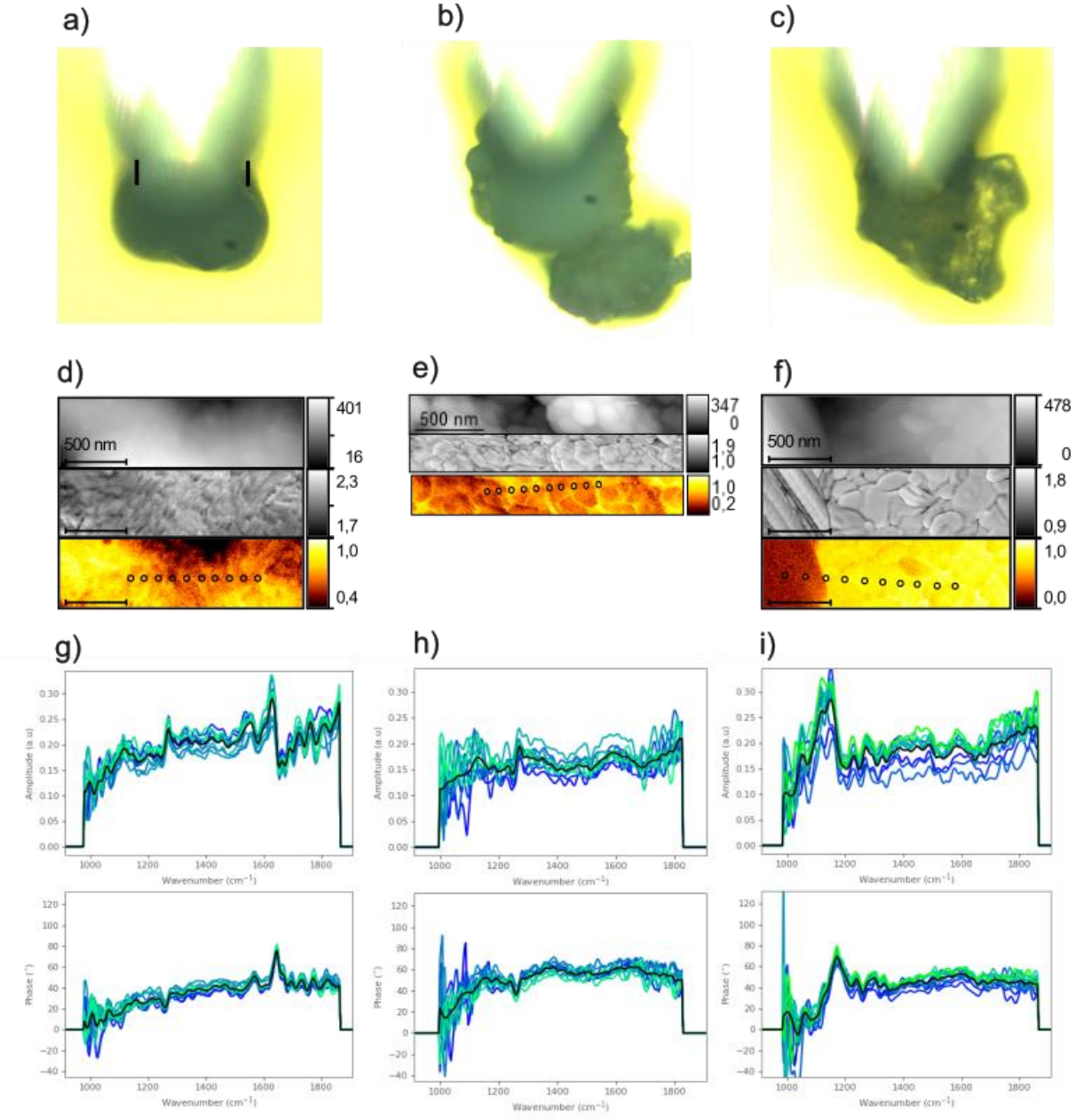

Figure S6 Optical microscope images of representative a) Nylon-12 b) PA-TP260 c) PA-**1** particles from filter samples on Au. Distance between black lines in panel a) is 50 µm. Panels d)-f) are local s-SNOM images of the top surface of particles in panels a) – c), where top panel is AFM height (scale nm), middle panel is tip 1st order mechanical phase change (scale rad.), and bottom panel is broadband optical scattering image of the surface (2nd order amplitude, scale norm.). Positions where nano-FTIR spectra have been measured are indicated in the bottom panels by black circles. Panels g)-i) show individual second order amplitude A_2 and phase φ_2 spectra taken from the indicated positions (green-blue spectra). Averaged spectra from different positions are shown with black lines.

Table S2 Elemental compositions (wt%) in NdFeB magnets determined by total dissolution using aqua regia.

Fe	Nd	Dy	Pr	Co	B	Tb	Sm	Ho	Al	Cu
63.21 ±1.30	21.03 ±0.35	2.70 ± 0.09	6.19 ± 0.20	0.92 ± 0.03	0.79 ± 0.08	0.18 ± 0.01	0.66 ± 0.02	0.46 ± 0.01	1.14 ± 0.09	0.38 ± 0.08

Table S3 Precipitation percentages in Fe(III) removal at pH 3.7.

Fe	Nd	Dy	Pr	Co	B	Tb	Sm	Ho	Al	Cu
99.6 ± 0.6%	3.5 ± 2.8%	3.4 ± 1.8%	3.6 ± 1.8%	3.6 ± 0.6%	0.0 ± 0.0%	3.1 ± 0.3%	3.5 ± 0.7%	3.1 ± 0.8%	27.3 ± 3.0%	11.9 ± 6.6%

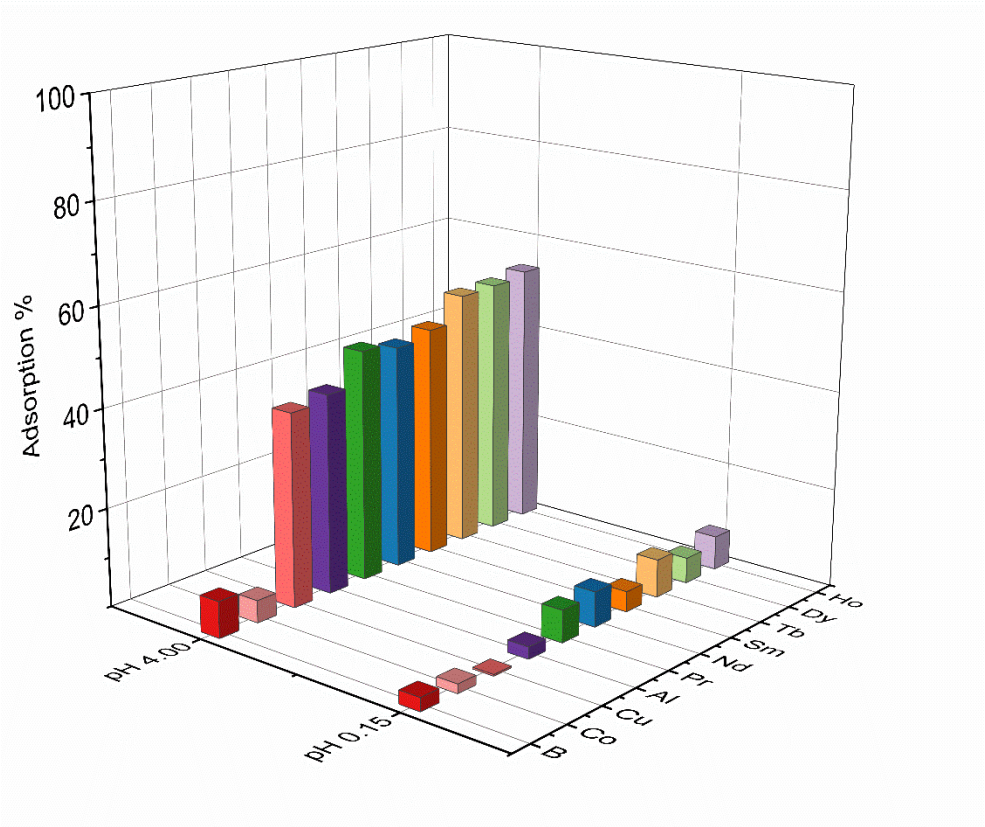

Figure S7 Adsorption percentages for the 30 wt% PA-**1** filter at pH 0.15 and pH 4.00

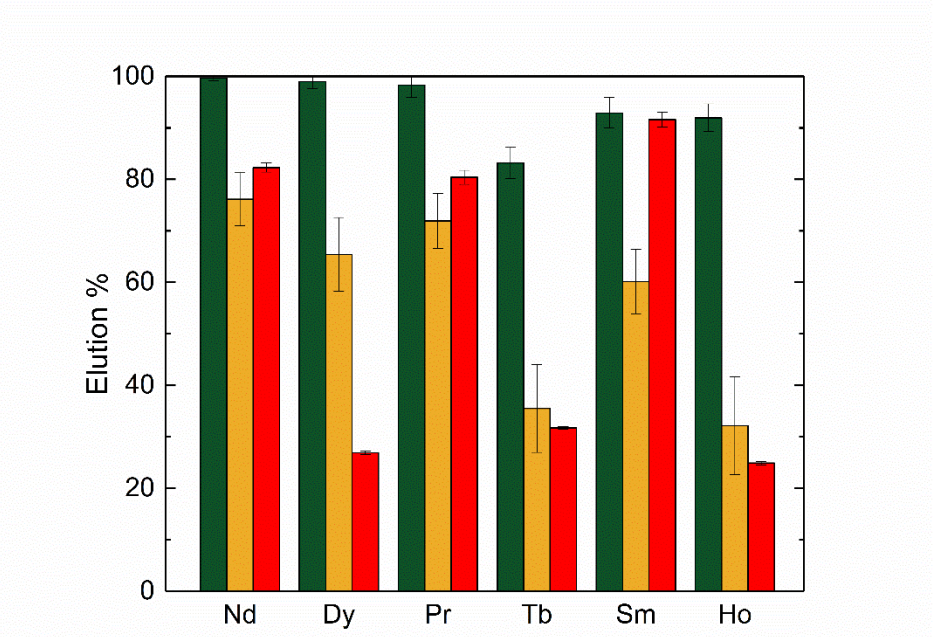

Figure S8 Desorption of REEs with 5 M MSA (green), 3 M MSA (yellow), and 6 M HNO_3 (red).

Table S4. Average amounts of all elements adsorbed by and desorbed from the filter and their standard deviations during the 50 adsorption–desorption cycles for every five cycles.

Cycle	Adsorption		Desorption	
	Average (mg/g)	Standard deviation (mg/g)	Average (mg/g)	Standard deviation (mg/g)
5	1,880	0,099	1,428	0,148
10	1,770	0,081	1,805	0,042
15	1,607	0,090	1,686	0,126
20	1,630	0,121	1,679	0,079
25	1,559	0,108	1,578	0,087
30	1,530	0,103	1,564	0,096
35	1,537	0,113	1,520	0,171
40	1,607	0,091	1,610	0,093
45	1,602	0,151	1,542	0,122
50	1,697	0,096	1,764	0,134

Table S5. Average amounts of elements adsorbed by three stacked filters (per single filter) in step 3 and desorbed from the filter in step 5 along with their standard deviations.

	Average (mg/g)	Standard deviation (mg/g)
Adsorbed (step 3)	1,631	0,441
Desorbed (step 5)	1,693	0,420

Table S6 Results for the image analysis during the 50 adsorption-desorption cycles

Number of cycles	Total porosity [%]	Average pore size [µm]	Standard deviation of the pore size [µm]	Average of the particle size distribution [µm]	Mode of the particle size distribution [µm]	Surface area [cm^2]	Connected porosity [%]
0 (Initial state)	50 ± 2	34 ± 5	13 ± 2	69 ± 5	51 ± 5	221 ± 10	99.994 ± 0.006
10	50 ± 2	33 ± 5	13 ± 2	68 ± 5	51 ± 5	223 ± 10	99.989 ± 0.006
20	50 ± 2	33 ± 5	13 ± 2	69 ± 5	51 ± 5	224 ± 10	99.991 ± 0.006
30	50 ± 2	33 ± 5	13 ± 2	68 ± 5	51 ± 5	227 ± 10	99.988 ± 0.006
40	50 ± 2	33 ± 5	13 ± 2	68 ± 5	51 ± 5	227 ± 10	99.987 ± 0.006
50	49 ± 2	32 ± 5	13 ± 2	69 ± 5	51 ± 5	227 ± 10	99.988 ± 0.006

.

zz

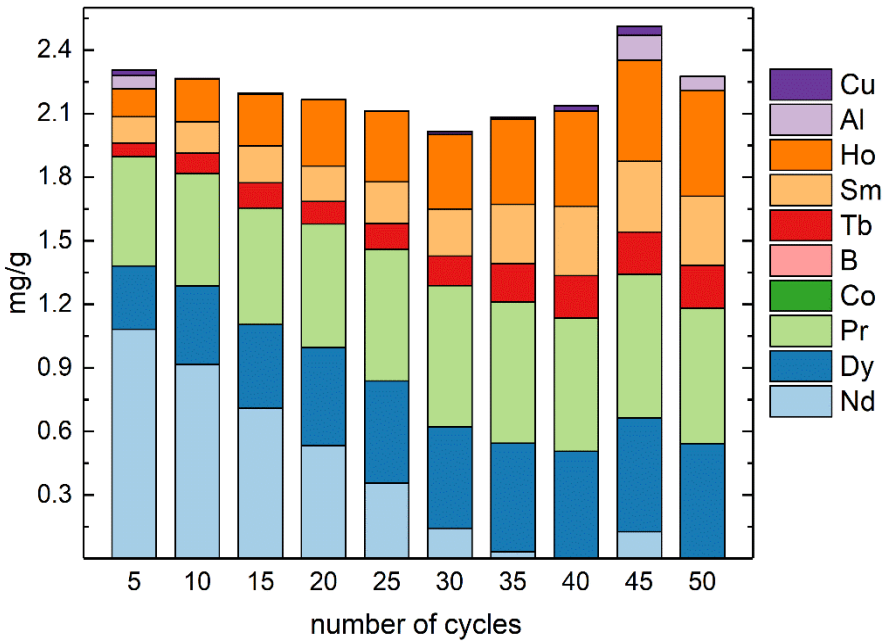

Figure S9 Residual amounts of elements in the PA-TP260 filter used in the 50 adsorption-desorption cycles.

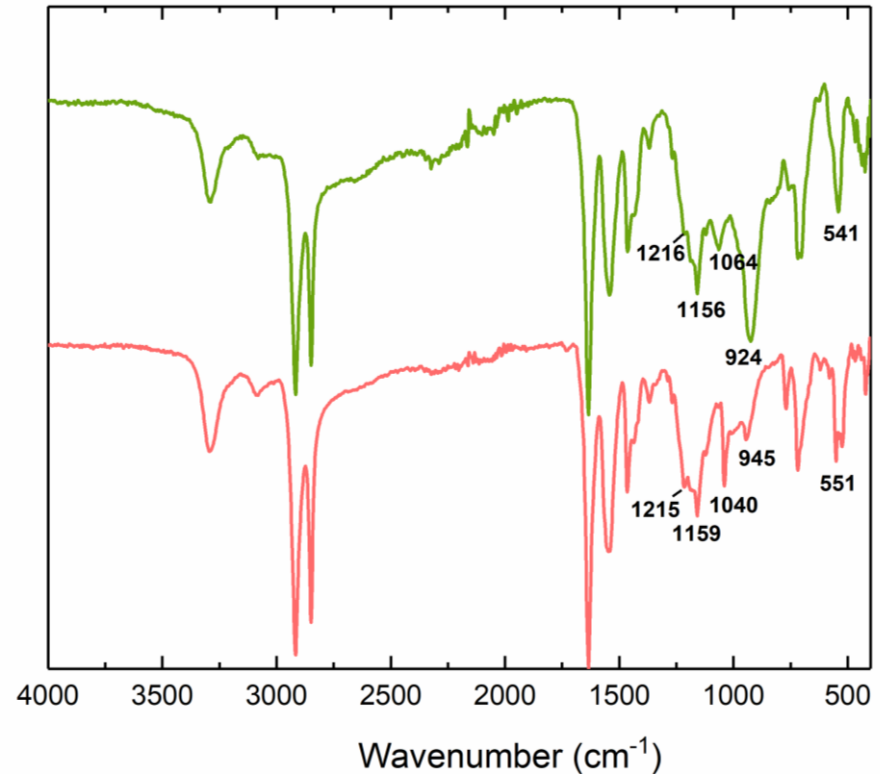

Figure S10. IR spectra of PA-TP260 filter used for the 50 adsorption-desorption cycles. Filter before the cycles above (green), and filter after the cycles below (pink).

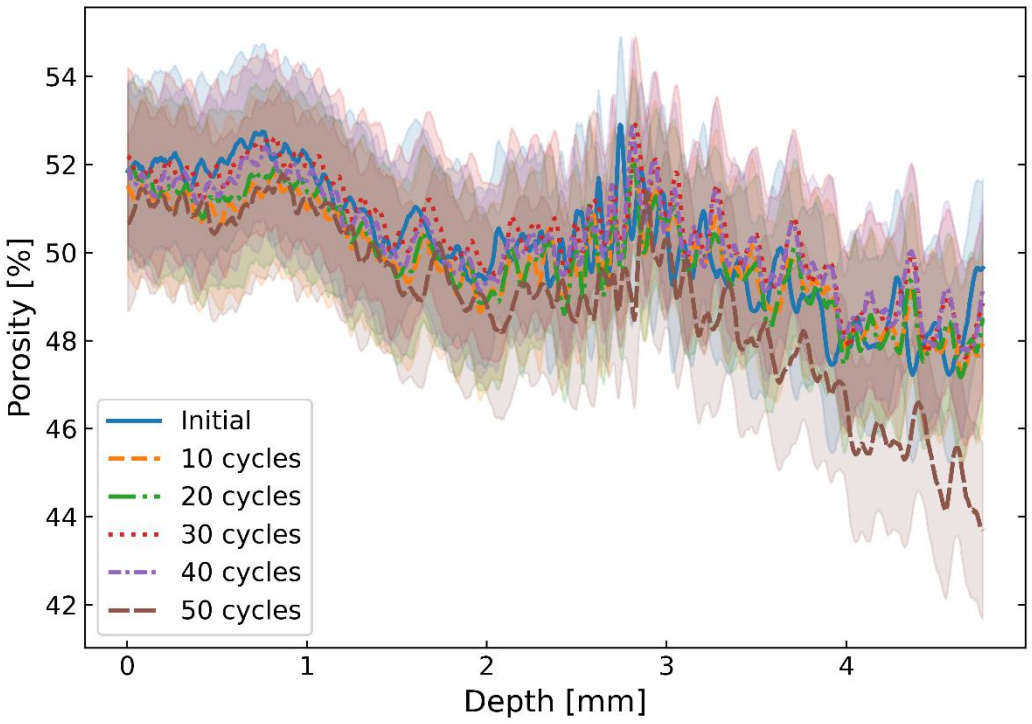

Figure S11 Depth profile of the porosity determined by image analysis during the adsorption desorption cycles. Error estimate (2%) is visualised as a shaded background with the corresponding colour.

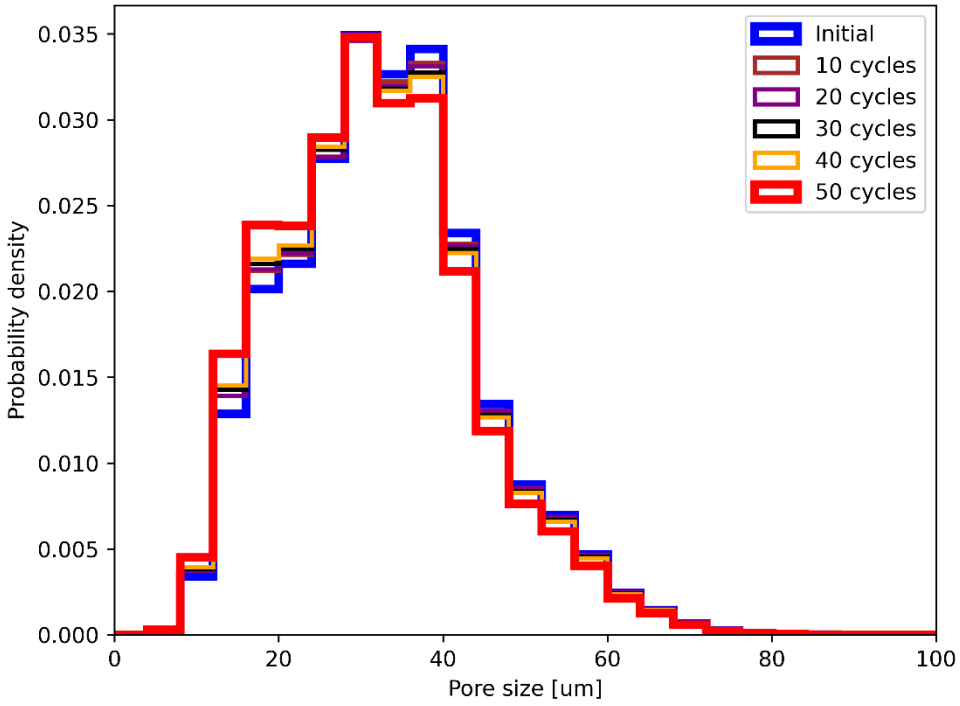

Figure S12 Pore size distribution according to the image analysis during the adsorption-desorption cycles

Table S7 Parameters for the Langmuir, Freundlich, and Sips adsorption isotherms as well as the obtained correlation coefficients R^2.

Model	Parameter	5%	10%	20%	30%	40%	50%
Langmuir	Q_m **mg/g filter**	-	7.64±2.17	9.71±2.41	9.12±0.75	10.09±0.50	12.18±0.86
	Q_m **mg/g TP260**	-	76.39±21.75	48.56±12.07	30.65±2.49	25.22±1.25	24.35±1.72
	B	-	1.60±0.62	2.53±1.15	5.47±1.47	7.10±1.02	11.30±1.28
	R^2	-	*0.992±0.006*	*0.987±0.004*	*0.985±0.004*	*0.972±0.007*	*0.957±0.017*
Sips	Q_m **mg/g filter**	2.55±0.23	5.82±1.59	-	-	-	-
	Q_m **mg/g TP260**	50.92±4.62	58.20±15.86	-	-	-	-
	b	3.97±0.70	2.60±0.91	-	-	-	-
	n	1.62±0.10	1.22±0.08	-	-	-	-
	R^2	*0.989±0.003*	*0.996±0.003*	-	-	-	-
Freundlich	K_f	0.03±0.01	0.05±0.02	0.13±0.10	-	0.71±0.13	1.33±0.13
	n	1.59±0.14	1.48±0.14	1.75±0.23	-	2.63±0.15	3.09±0.17
	R^2	*0.938±0.012*	*0.975±0.013*	*0.982±0.012*	-	*0.997±0.001*	*0.993±0.003*

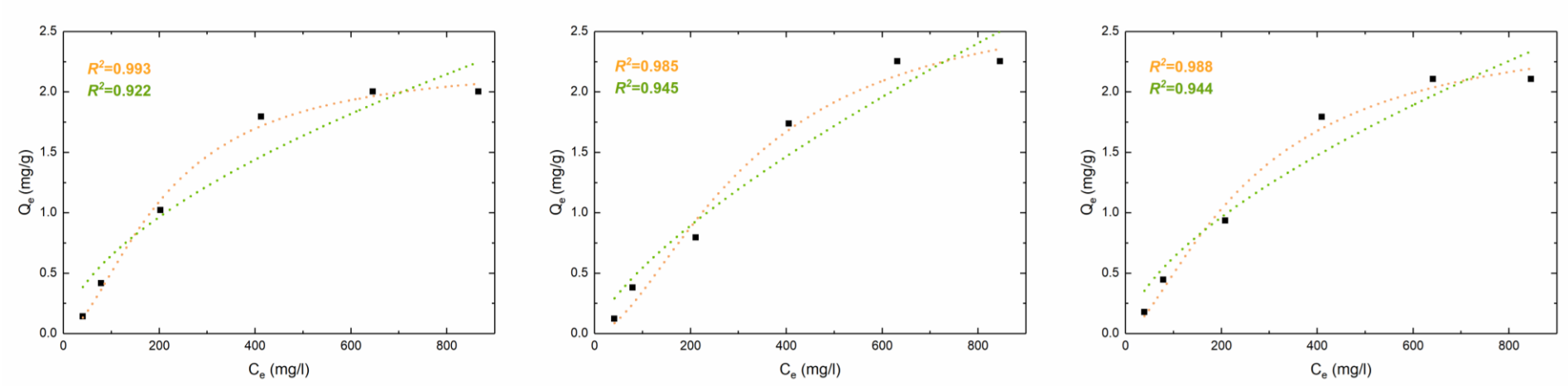

Figure S13 Adsorption isotherm fittings for the 5 wt% PA-TP260 filter with Nd. Orange is Sips isotherm and green is Freundlich isotherm. The Langmuir model did not fit to isotherm.

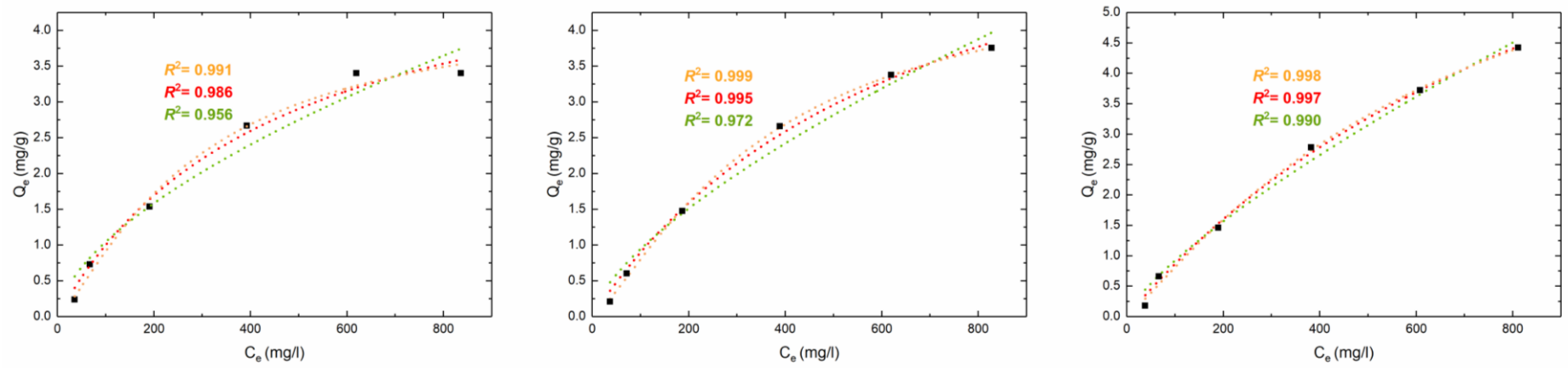

Figure S14 Adsorption isotherm fittings for the 10 wt% PA-TP260 filter with Nd. Sips isotherm in orange, Freundlich isotherm in green, and Langmuir isotherm in red.

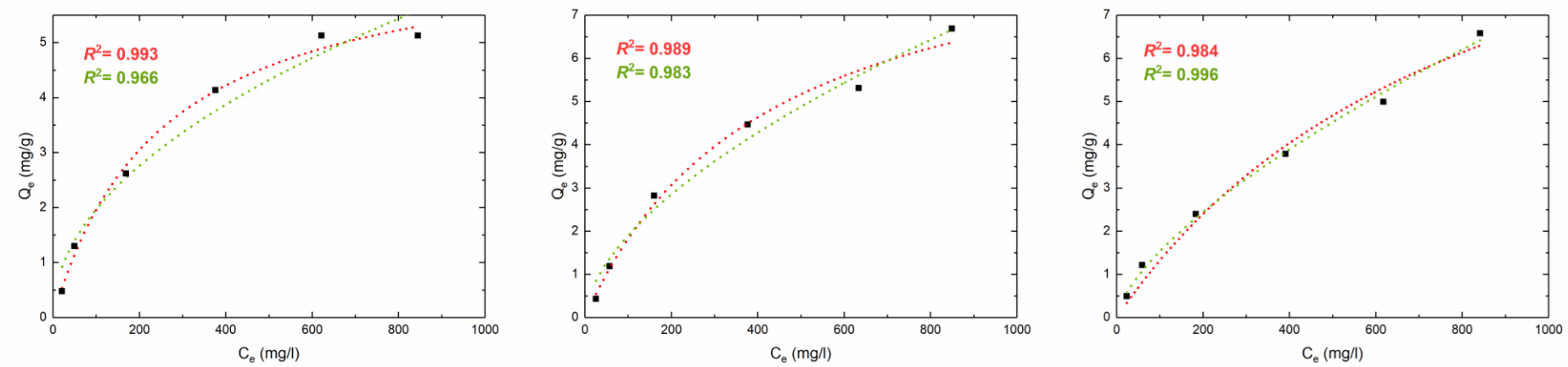

Figure S15 Adsorption isotherm fittings for the 20 wt% PA-TP260 filter with Nd. Freundlich isotherm in green and Langmuir isotherm in red. The Sips model did not fit to isotherm.

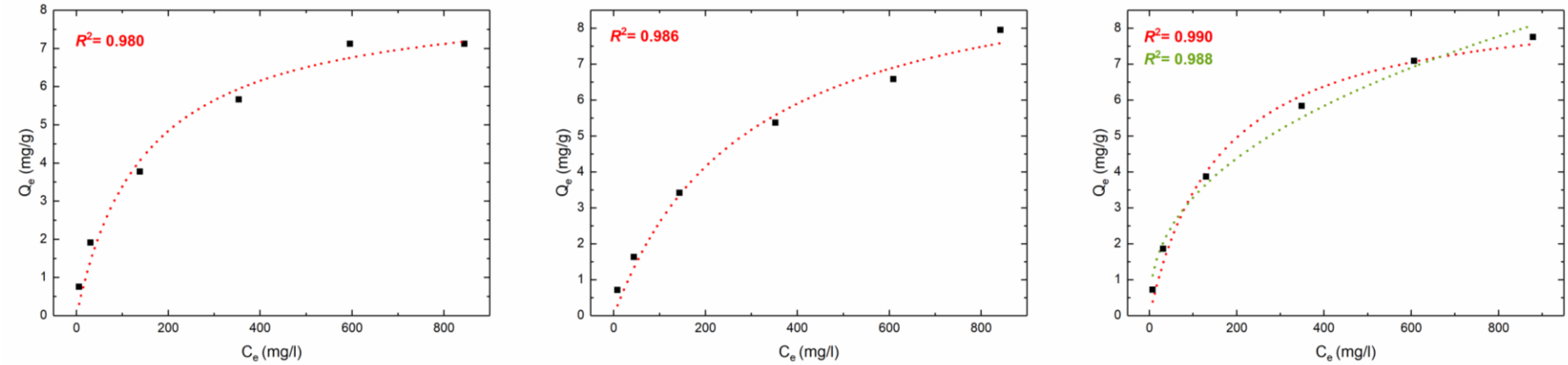

Figure S16 Adsorption isotherm fittings for the 30 wt% PA-TP260 filter with Nd. Freundlich isotherm in green and Langmuir isotherm in red. Only one replicates fit successfully to the Freundlich model, whereas the Sips model did not fit to isotherm.

.

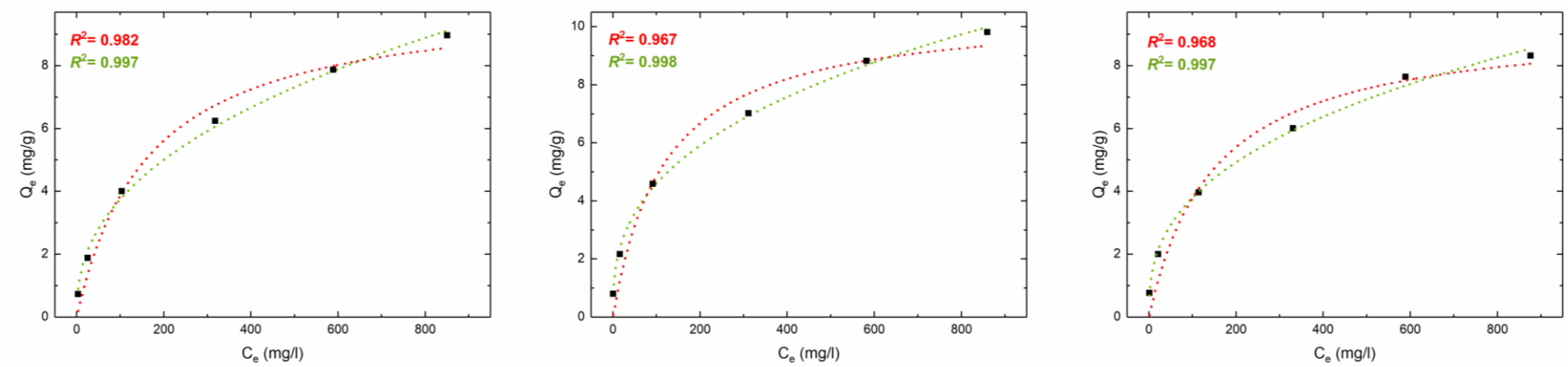

Figure S17 Adsorption isotherm fittings for the 40 wt% PA-TP260 filter with Nd. Freundlich isotherm in green and Langmuir isotherm in red. The Sips model did not fit to isotherm.

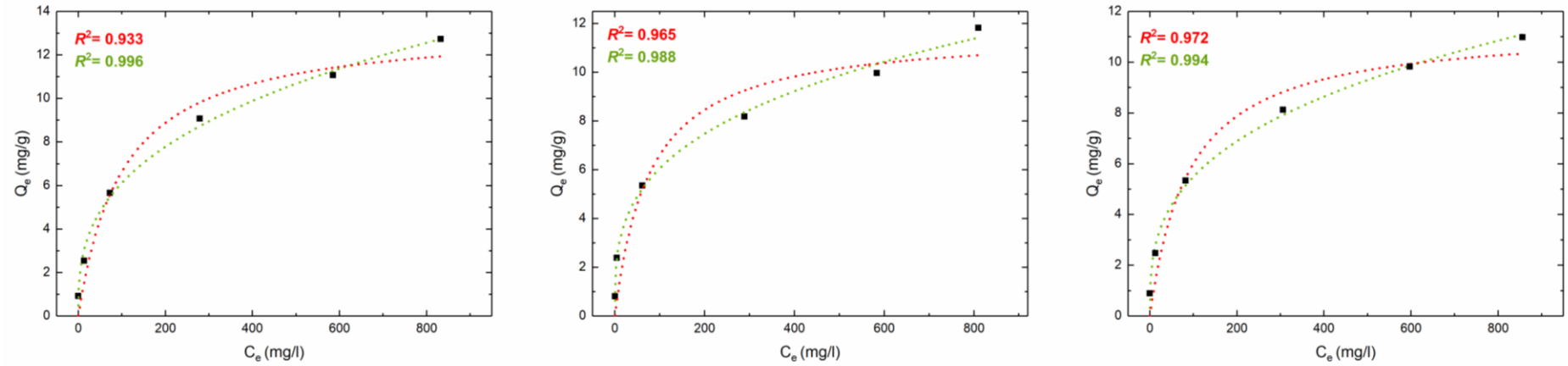

Figure S18 Adsorption isotherm fittings for the 50 wt% PA-TP260 filter with Nd. Freundlich isotherm in green and Langmuir isotherm in red. The Sips model did not fit to isotherm.

Table S8 Maximum adsorption capacities Q_m for Nd^{3+} reported for the aminophosphonate-based adsorbents.

Adsorbent	Q_m	**pH**	**ref**
Aminobisphosphonate (PA-1)	34.60 mg/g	4	[4]
Commercial aminophosphonate functionalised resin Purolite S950	98.44 mg/g	-	[5]
Aminophosphonate functionalized PGMA	111.93 mg/g	4.5	[6]
Aminophosphonic functionalized chitosan	30.32 mg/g	5	[7]
Monoaminophosphonate	184.92 mg/g	4.5	[8]
Bisaminophosphonate	202.66 mg/g	4.5	[8]

Table S9. Adsorption %, elution %, and amount in µg for each step of the separation process.

Step 3	**Nd**	**Dy**	**Pr**	**Co**	**B**	**Tb**	**Sm**	**Ho**	**Al**	**Cu**
Adsorption %	99.9±0.1%	100.0±0.0%	99.5±0.5%	1.1±1.2 %	3.9±4.0 %	100.0±0.0%	99.8±0.3%	100.0±0.0%	37.8±8.8%	30.3±17.2%
Adsorbed in µg	561.2±149.3	70.9±17.0	170.2±40.2	0.2±0.2	0.6±0.6	5.5±1.5	15.3±4.3	10.9±3.1	7.0±1.6	1.4±0.6
Step 3.1	**Nd**	**Dy**	**Pr**	**Co**	**B**	**Tb**	**Sm**	**Ho**	**Al**	**Cu**
Adsorption %	-	-	-	45±8%	10±10 %	-	-	-	100.0±0.0%	93±8%
Adsorbed in µg	-	-	-	8.1±2.6	1.1±1.1	-	-	-	10.7±3.7	2.9±1.1
Passed through %	-	-	-	55.4±7.7%	89.7±10.2%	-	-	-	-	7.5±7.7 %
Passed through µg	-	-	-	11.2±3.2	22.7±13.5	-	-	-	-	0.3±0.3
Step 3.2	**Nd**	**Dy**	**Pr**	**Co**	**B**	**Tb**	**Sm**	**Ho**	**Al**	**Cu**
Elution %	-	-	-	56.3±16.4%	-	-	-	-	-	27.7±15.3%
Eluted in µg	-	-	-	4.1±0.4	-	-	-	-	-	0.6±0.2
Step 3.3	**Nd**	**Dy**	**Pr**	**Co**	**B**	**Tb**	**Sm**	**Ho**	**Al**	**Cu**
Elution %	-	-	-	37.7±7.8%	-	-	-	-	99.1±1.5%	65.0±24.6%
Eluted in µg	-	-	-	3.0±0.9	-	-	-	-	13.5±4.2	2.0±0.7
Step 4	**Nd**	**Dy**	**Pr**	**Co**	**B**	**Tb**	**Sm**	**Ho**	**Al**	**Cu**
Elution %	-	-	-	-	-	-	-	-	-	57.2±26.0%
Eluted in µg	-	-	-	-	-	-	-	-	-	1.0±0.4
Step 5	**Nd**	**Dy**	**Pr**	**Co**	**B**	**Tb**	**Sm**	**Ho**	**Al**	**Cu**
Elution %	99.8±0.4%	74.6±8.6%	99.7±0.3%	-	-	64.2±19.4%	99.8±0.3%	75.4±6.6%	95.8±0.4	99.7±0.5
Eluted in µg	599.2±148.6	54.2±18.2	180.8±42.6	-	-	3.8±2.0	16.8±4.5	8.4±2.8	6.9±1.7	0.3±0.1

References

1. Larkin, P. *Infrared and Raman Spectroscopy: Principles and Spectral Interpretation*. (Elsevier, San Diego, UNITED STATES, 2011).
2. Stuart, B. H. *Infrared Spectroscopy: Fundamentals and Applications*. (John Wiley & Sons, Incorporated, Newark, UNITED KINGDOM, 2004).
3. Sahni, S. K., Van Bennekom, R. & Reedijk, J. A spectral study of transition-metal complexes on a chelating ion-exchange resin containing aminophosphonic acid groups. *Polyhedron* **4**, 1643–1658 (1985).
4. Virtanen, E. J. *et al.* Recovery of rare earth elements from mining wastewater with aminomethylphosphonic acid functionalized 3D-printed filters. *Separation and Purification Technology* **353**, 128599 (2025).
5. Burdzy, K., Ju, Y. & Kołodyńska, D. Iminodisuccinic acid (IDHA) as an effective biodegradable complexing agent in the adsorption process of La(III), Nd(III) and Ho(III) ions. *Chemical Engineering Journal* **461**, 142059 (2023).
6. Galhoum, A. A. *et al.* Functionalization of poly(glycidylmethacrylate) with iminodiacetate and imino phosphonate groups for enhanced sorption of neodymium - sorption performance and molecular modeling. *Reactive and Functional Polymers* **180**, 105389 (2022).
7. Elsalamouny, A. R., Desouky, O. A., Mohamed, S. A., Galhoum, A. A. & Guibal, E. Uranium and neodymium biosorption using novel chelating polysaccharide. *International Journal of Biological Macromolecules* **104**, 963–968 (2017).
8. Imam, E. A. *et al.* Nd(III) sorption using aminophosphonate-based sorbents – Sorption properties and application to the treatment of REE concentrate. *Colloids and Surfaces A: Physicochemical and Engineering Aspects* **685**, 133339 (2024).